



# Piconet construction and restructuring mechanisms for interference avoiding in bluetooth PANs



Qiaoyun Zhang<sup>a</sup>, Guilin Chen<sup>a,c</sup>, Liang Zhao<sup>a</sup>, Chih-Yung Chang<sup>b,\*</sup>

<sup>a</sup> Chuzhou University, Chuzhou, China

<sup>b</sup> Tamkang University, Taiwan

<sup>c</sup> Anhui Center for Collaborative Innovation in Geographical Information Integration and Application, Chuzhou

## ARTICLE INFO

### Article history:

Received 21 July 2015

Received in revised form

30 May 2016

Accepted 22 August 2016

Available online 27 August 2016

### Keywords:

Interference

Bluetooth

Wi-Fi

## ABSTRACT

Bluetooth and IEEE 802.11 (Wi-Fi) are two of the most popular communication standards that define physical and MAC layers for wireless transmissions and operate on 2.4 GHz industrial scientific medical (ISM) band. To avoid the rich interference existed in ISM band, Bluetooth adopts a time-slotted frequency-hopping spread-spectrum scheme, preventing the Bluetooth device communication from being interfered for a long time on specific channel. However, the coexistence of Bluetooth and Wi-Fi in the neighborhood degrades the performance of both networks because the two wireless technologies cannot negotiate with each other. To improve the throughput of a given piconet, this paper presents two interference aware approaches. First, an interference aware piconet establishment mechanism, called *IAPE*, is proposed to consider the frequencies occupied by Wi-Fi and then minimize the interference from Wi-Fi transmissions, when Bluetooth and Wi-Fi coexist in the same space. To further improve the throughput of the constructed piconet, an interference aware piconet restructuring mechanism, called *IAPR*, is proposed. Performance study reveals that the proposed *IAPE* and *IAPR* approaches further reduce the interference between Bluetooth and Wi-Fi and thereby save the energy of Bluetooth device, improving the throughput of Bluetooth personal area networks (PANs).

© 2016 Elsevier Ltd. All rights reserved.

## 1. Introduction

Bluetooth is a wireless technology, characterized by low power, low-cost, and short-range and operated on 2.4 GHz industrial scientific medical (ISM) band ([The Bluetooth Specification](#)). Bluetooth has been widely embedded in a variety of electronic devices such as printers, mobile phones, laptops, home video and audio systems, as well as sphygmomanometers, supporting short-range wireless communications ([Wang and Iqbal 2006](#); [Abdullah and Poh, 2011](#)). To avoid the rich interference existed in ISM band, it adopts a time-slotted frequency-hopping spread-spectrum scheme with a forward error correction (FEC) coding technique. The Bluetooth signal occupies 1 MHz bandwidth and changes center frequency (or hops) deterministically at a rate of 1600 Hz. Bluetooth hops over 79 center frequencies, equally spaced between 2.402 GHz and 2.480 GHz ([Ophir et al., 2004](#); [Gummadi et al., 2007](#)). A piconet is the smallest network element that

consists of a master device and slave devices (up to seven). Each piconet has its own hopping sequence that determines the communication channel in each time slot. In a piconet, the master and slave devices play the sender role and transmit packets in the even and odd slots, respectively. The transmission rate reaches up to 1 Mbps while the transmission range generally ranges from 10 m to 100 m, depending on the transmission power ([Lee et al., 2007](#)).

In the Bluetooth technology, interference from the other Bluetooth devices has been minimized because each piconet uses its own pseudo-random frequency-hopping pattern. However, several wireless technologies also share the ISM band, including Wi-Fi, ZigBee and others. In particular, the coexistence of Bluetooth and Wi-Fi degrades the network performance because the two wireless technologies cannot negotiate with each other. A single active Wi-Fi network causes the heavy interference on 37% of the Bluetooth channels ([Lavric et al., 2012](#)). Therefore, an open question in Bluetooth is how to avoid interference conflicts among devices, which try to simultaneously access a Bluetooth personal area network (PAN) or Wi-Fi network.

Previous work ([Jeon et al., 2013](#)) proposed an approach to avoid the in-device interference when Wi-Fi and Bluetooth radios coexisted simultaneously in the same device. In ([Jeon et al., 2013](#)), a

\* Corresponding author.

E-mail addresses: [zqyun@chzu.edu.cn](mailto:zqyun@chzu.edu.cn) (Q. Zhang), [glichen@chzu.edu.cn](mailto:glichen@chzu.edu.cn) (G. Chen), [leon@chzu.edu.cn](mailto:leon@chzu.edu.cn) (L. Zhao), [cychang@mail.tku.edu.tw](mailto:cychang@mail.tku.edu.tw) (C.-Y. Chang).

canceler was introduced in the circuit to prevent the interference. However, study (Jeon et al., 2013) did not take the interference into consideration when the Bluetooth and Wi-Fi devices had coexisted in different devices.

Heterogeneous interference, such as Wi-Fi and Bluetooth co-existence, had various characteristics and properties (Lakshminarayanan et al., 2011). In order to reduce the interference, Baccour et al. (2012) proposed a mechanism based on the estimation of radio link quality to reduce the heterogeneous interference in wireless sensor networks (WSNs). The coexistence problems could be detected by the link quality estimator. However, the link quality estimation needed to send a considerable amount of control messages to make a decision whether or not the interference exists. This raised many overheads, leading to the poor performance regarding the throughput.

To mitigate the phenomenon of the co-channel interference in the Bluetooth piconet, studies (Yoon et al., 2010; Lee et al., 2012) proposed approaches to check whether or not the next channel for the Bluetooth frequency hopping was occupied by the other signals. Lee et al. (2012) proposed a mechanism that periodically detected busy channels subject to the WLAN interference. The proposed mechanism evaluated the packet error rate and the interference signal detection rate before sending packets. However, this approach needed to periodically check every channel, leading to the considerable energy consumption. In addition, the scheme did not deal with the packet retransmission problem caused by the WLAN interference, further increasing the time and energy costs of packet retransmissions.

There have been many works on the Bluetooth role switch, but they are tending to propose a role switch formation protocols for constructing a proper scatternet. Study (Chang and Chang, 2006) can remove unnecessary bridges and the piconet using role switch to improve the packet error rate and reduce the average length. Study (Bakhsh et al., 2012) presents a flexible relay selection technique to reduce unnecessary relays. However, they didn't consider to how to restructure a piconet dynamically when the master of Bluetooth piconet suffers the interference from Wi-Fi devices.

Study (Chiasserini and Rao, 2002) proposed two coexistence mechanisms, including V-OLA and D-OLA in the presence of a Bluetooth voice link and Bluetooth data link, respectively. In the V-OLA mechanism, whenever a 802.11 station is ready to transmit, it detects whether or not the channel is idle. If it is the case, the 802.11 station expects for a time period that there is no BT transmission and transmits a data packet within the expected time period. Conversely, if the channel is occupied by an interfering signal, the WLAN station can either (i) send a packet with a 500 bytes payload (Shortened Transmission (ST) mode) or (ii) refrain from transmitting (Postponed Transmission (PT) mode). In the D-OLA mechanism, a BT device can identify the frequency channels that are occupied. According to the D-OLA algorithm, if enough data are buffered at the master for the intended slave, the master schedules a multi-slot packet instead of a single-slot packet, aiming to skip the channels that are occupied by WLAN. The scheduling algorithm could also let the master (slave) refrain from transmitting in the time slot corresponding to a frequency that hops on the 802.11 band whenever there are not enough data in the buffer at the master. Though the proposed V-OLA and D-OLA mechanisms can avoid the collision occurrence, the throughput and packet delay can be further improved. For example, the D-OLA will not allow the master to transmit data to slave at the next time slot if the working channel of hopping sequence is busy at the next time slot. However, our mechanism can utilize the next time slot to transmit data if the role of master has been changed to the slave. As a result, the packet delay and throughput can be improved. The following compares the proposed mechanism and the

mechanisms proposed in (Chiasserini and Rao, 2002). First of all, in the connection process, the proposed mechanism *IAPE* tries to scan the channels that are occupied by 802.11. The constructed piconet will skip these channels in the hopping sequence. Therefore, no further detection is needed whether the piconet has been constructed. Hence, all time slots can be used for transmitting data, reducing the delay and improving the throughput. Second, the proposed mechanism *IAPR* actively reconstructs the piconet and the device that can minimize the transmission delay and maximal throughput will be invited to be the new master when the retransmission rate reaches the threshold. The proposed mechanism dynamically changes the piconet structure and thus can be further applied to the mobile network.

This paper presents a novel Bluetooth network construction mechanism that explores appropriate channels during link construction and reconstructs the piconet topology during data transmission for Bluetooth network, aiming at minimizing the interference between Bluetooth and Wi-Fi when they coexist in the same space. The contributions of this paper are itemized as follows:

- (1) *Avoiding the interference during Bluetooth link construction.*  
The proposed interference aware piconet establishment (*IAPE*) mechanism constructs an efficient Bluetooth link by exploring the appropriate channels such that the hopping sequence skips the channels occupied by Wi-Fi.
- (2) *Reducing the network overheads raised by packet transmissions.*  
This paper proposes an interference aware piconet restructuring mechanism (*IAPR*), which applies the role switching operations to restructure a new piconet. The reconstructed Bluetooth network reduces the phenomenon of packet retransmission and hence substantially reduces the network overheads.
- (3) *Reducing the energy consumption and the transmission delay for Bluetooth networks.*

The time and energy costs of packet retransmissions are improved because of the lower collision rate achieved by the proposed scheme. Hence the energy consumptions of Bluetooth devices can be saved.

The remaining part of this paper is organized as follows. Section II illustrates the network environment and formulates the problem investigated in this paper while Sections III and IV elaborate the proposed *IAPE* and *IAPR* mechanisms, respectively. Section V verifies the performance of the proposed mechanisms by MATLAB simulation. Finally, Section VI offers a conclusion.

## 2. Network environment and problem statement

To achieve the readability, Table 1 lists a set of notations that are used in this paper.

### 2.1. Network environment

Assume that there are  $m$  Wi-Fi devices represented by  $W = \{w_1, w_2, \dots, w_m\}$  and  $n$  Bluetooth devices represented by  $B = \{b_1, b_2, \dots, b_n\}$  coexist in the same space.

The following communication model is applied in this paper. The signal strength  $P^{rx}$  at receiver side is modeled by Exp. (1), where  $P^{tx}$  is the transmitter power,  $G^{tx}$  and  $G^{rx}$  are antenna gains of the transmitter and receiver,  $\eta$  is referred to as rectifier efficiency,  $L^p$  denotes the polarization loss,  $\mu$  is the wavelength of RF wave,  $d$  is the distance between a sender and the corresponding receiver, and  $\sigma$  denotes an adjustable parameter to adapt our equation to

**Table 1**  
Notation List.

Notation	Definition
$W$	A set of Wi-Fi devices, $W = \{w_1, w_2, \dots, w_m\}$
$B$	A set of Bluetooth devices, $B = \{b_1, b_2, \dots, b_n\}$
$p^{tx}, p^{rx}$	Transmitter power and the power at the receiver
$G^{tx}, G^{rx}$	Antenna gains of the transmitter and the receiver
$d$	Distance between the transmitter and the receiver
$\mu$	Wavelength of the RF wave
$\eta$	Rectifier efficiency
$L^P$	Polarization loss
$\sigma$	An adjustable parameter to adapt Exp. (1) to room environment
$\tau$	A constant that $\tau = (G^{tx}G^{rx}\eta/L^P)(\lambda/4\pi)^\gamma$
$I_{(b_j, H_j, w_i)}^T$	The interference at Bluetooth device $b_j$ generated by the Wi-Fi device $w_i$ during the period $T$ by adopting the hopping sequence $H_j$
$d_{ij}$	Distance between Wi-Fi device $w_i$ and Bluetooth device $b_j$
$\alpha_j^t$	Boolean variable, which represents whether or not the Bluetooth device $b_j$ is a receiver in a time slot $t$ .
$\vartheta_s^t, \vartheta_r^t, \vartheta_{idle}^t$	Sending, receiving and idle listening data of device $b_\theta$ at time slot $t$ , respectively.
$\vartheta_{master}^t, \vartheta_{slave}^t, \vartheta_{bridge}^t$	Master, slave and bridge device at time $t$ , respectively.
$\vartheta_{master}^{even}$	Device $b_\theta$ sending packet initially at even time slot when $b_\theta$ plays a master role
$\vartheta_{slave}^{odd}$	Device $b_\theta$ sending packet initially at odd time slot when $b_\theta$ plays a slave role
$c_j^t$	the channel of the hopping sequence $H_j$ at time slot $t$ .
$\delta$	The time for handling the signal received from Wi-Fi signal
$\lambda$	Threshold of signal strength
$\varphi_q$	The signal strength on the scanned channel $c_q$
$\beta_q$	A Boolean variable indicating whether $\varphi_q > \lambda$
$A_j$	Address of device $b_j$
$H_j^{type}$	The device $b_j$ adopts universal hopping sequence ( $type = universal$ ) or the hopping sequence generated based on the address $A_j$ ( $type = A_j$ )
$\pi(H_j, speed)$	The device $b_j$ adopts hopping sequence $H_j$ with a speed "fast" or "slow"
$\omega_j$	Clock stamp in an FHS packet when $b_j$ transmits the FHS packet
$Table^{b_{master}}$	A table maintained by master $b_{master}$ , recording every slave host's interference channels
$R_\theta$	Threshold of packet retransmissions
$S_{succ}$	A set of most recent received packets of master $b_{master}$ . $S_{succ} = \{s_1, s_2, \dots, s_y\}$
$r_u$	Retransmission number of the packet $s_u$
$\bar{r}_{master}$	The average retransmission number of the most recent $y$ packets, which are successfully received by $b_{master}$
$C$	a piconet
$l_{ij}$	Link between devices $b_i$ and $b_j$
$F_{ij}^a$	Flow data volume from $b_i$ to $b_j$ in a piconet where $b_a$ is the master
$p_{ij},  p_{ij} $	A path from device $b_i$ to device $b_j$ with the length $ p_{ij} $
$f_{ij}^1, f_{ij}^2$	Two flow data volumes from slave $b_i$ to master $b_a$ and from master $b_a$ to slave $b_j$ , respectively
$r_{ij}^1, r_{ij}^2$	Two retransmission numbers from slave $b_i$ to master $b_a$ and from master $b_a$ to slave $b_j$ , respectively
$F_a$	Total flow data volume of master $b_a$
$\gamma^a$	Piconet restructuring benefit of master $b_a$

room environment.

$$p^{rx} = \frac{G^{tx}G^{rx}\eta}{L^P} \left( \frac{\mu}{4\pi(d+\sigma)} \right)^\gamma p^{tx} \quad (1)$$

where  $\gamma$  denotes an exponential index ranging from 2 to 4. Afterward, Exp. (1) is further simplified as Exp. (2), where  $\tau = (G^{tx}G^{rx}\eta/L^P)(\mu/4\pi)^\gamma$  is a constant.

$$p^{rx} = \frac{\tau}{(d+\sigma)^\gamma} p^{tx} \quad (2)$$

## 2.2. Problem formulation

Let  $I_{(b_j, c_q)}^{w_i}$  denote the interference at Bluetooth device  $b_j$  generated by the Wi-Fi device  $w_i$  on the channel  $c_q$ . Let  $d_{ij}$  denote the distance of a Wi-Fi device  $w_i$  and a Bluetooth device  $b_j$ . Let  $P^{w_i}$  denote the transmitter power of Wi-Fi device  $w_i$ . Because the fact that the received signal strength of Bluetooth device  $b_i$  from the Wi-Fi device  $w_i$  is equal to the interference signal strength which Bluetooth device  $b_i$  suffered from the Wi-Fi device  $w_i$ , we have

$$I_{(b_j, c_q)}^{w_i} = \frac{\tau}{(d_{ij} + \sigma)^\gamma} P^{w_i} \quad (3)$$

Let  $\alpha_j^t$  denote a Boolean variable, which represents whether or not the Bluetooth device  $b_j$  is a receiver in a time slot  $t$ . That is,

$$\alpha_j^t = \begin{cases} 1, & \text{if } b_j \text{ is a receiver in a time slot } t \\ 0, & \text{otherwise} \end{cases} \quad (4)$$

Let  $I_{(b_j, H_j, w_i)}^T$  denote the accumulated interference, which is caused from the Wi-Fi sender  $w_i$  at Bluetooth device  $b_j$  during the period  $T$  by adopting the hopping sequence  $H_j$ . Let  $c_j^t$  denote the channel of the hopping sequence  $H_j$  at time slot  $t$ . As a result, the interference at Bluetooth  $b_j$  from the Wi-Fi device  $w_i$  during the period  $T$  is represented in Exp. (5).

$$I_{(b_j, H_j, w_i)}^T = \sum_{\forall t \in T} \left( \alpha_j^t \times I_{(b_j, c_j^t)}^{w_i} \right) \quad (5)$$

This paper aims at choosing a proper hopping sequence and constructing piconets where each device  $b_j$  such that the total interference in these piconets accumulated during a given time period  $T$  is minimized, as depicted in Exp. (6).

$$\text{minimize } \sum_{j=1}^n \sum_{i=1}^m I_{(b_j, H_j, w_i)}^T \quad (6)$$

Let  $\vartheta_s^t, \vartheta_r^t, \vartheta_{idle}^t$  denote sending, receiving and idle listening data of device  $b_\theta$  at time slot  $t$ , respectively. Since each Bluetooth device has a single half-duplex antenna, the following presents the *Antenna Constraint*.

- **Antenna Constraint:**

The state of Bluetooth device  $b_\theta$  can only be one of sending, receiving or idle listening. That is,

$$\vartheta_s^t + \vartheta_r^t + \vartheta_{idle}^t = 1, \forall b_\theta \in B$$

Let  $\vartheta_{master}^t, \vartheta_{slave}^t, \vartheta_{bridge}^t$  denote master, slave and bridge device at time  $t$ , respectively. The following further presents the *Role Switch Constraint*.

- **Role Switch Constraint:**

In Bluetooth scatternet topology, device  $b_\theta$  can be only master, slave or bridge device at time  $t$ . That is,

$$\vartheta_{master}^t + \vartheta_{slave}^t + \vartheta_{bridge}^t = 1, \forall b_\theta \in B$$

Let  $\vartheta_{master}^{even}$  denote device  $b_\theta$  sending packet initially at even time slot when  $b_\theta$  plays a master role in a piconet. Let  $\vartheta_{slave}^{odd}$  denote device  $b_\theta$  sending packet initially at odd time slot when  $b_\theta$  plays a slave role. The following presents the *Sending Packet*

Constraint.

• **Sending Packet Constraint:**

The master and slave sending packet should follow the following constraints. That is, the master can only send data at even time slot, while each slave can only send data at odd time slot.

$$s_{master}^{even} = \begin{cases} 1, & \text{master } b_{\theta} \text{ send packet initially at even time slot} \\ 0, & \text{otherwise} \end{cases}$$

$$s_{slave}^{odd} = \begin{cases} 1, & \text{slave } b_{\theta} \text{ send packet initially at odd time slot} \\ 0, & \text{otherwise} \end{cases}$$

**3. Interference Aware Piconet Establishment (IAPE) mechanism**

This section presents the proposed novel Bluetooth connection protocol. In Bluetooth networks, a piconet is the basic networking unit. Bluetooth and Wi-Fi technologies share the same unlicensed ISM band in a piconet. As shown in Fig. 1, in a piconet, a master device and slave devices (up to seven) hop over 79 center channels, which are equally spaced between 2.402 GHz and 2.480 GHz, occupy the non-overlapped 1 MHz bandwidth. Similar to the Bluetooth standard, the Wi-Fi standard also operates on the frequency band ranging from 2.4 GHz to 2.4835 GHz, which is equally partitioned into several channels, each of which has 22 MHz bandwidth. Because the adjacent Wi-Fi channels are overlapped with each other, the transmissions arranged on adjacent channels will collide with each other, leading to the interference and packet retrasmmissions. For this reason, Wi-Fi APs are typically operated on channels 1, 6 and 11 to prevent the interference. In such scenario, three neighboring networks occupy approximately  $3 \times 22 \text{ MHz} = 66 \text{ MHz}$  of the available 83.5 MHz in the ISM band.

In a piconet, a master device, represented by  $b_{master}$ , is able to connect with slave hosts (up to seven), which are represented by  $b_1, b_2, \dots, b_7$ , respectively. As specified in the Bluetooth standard, the master and slaves initially stay in the inquiry state and inquiry scan state, respectively. Fig. 2 presents the whole connection procedure developed in this paper. To be aware the frequencies used by Wi-Fi, as shown in Fig. 2, each slave initially scans all the channels, aiming at detecting the interference caused from Wi-Fi transmissions. The detection duration on each channel should be at least  $\text{PIFS} + \delta$  to ensure that any existing Wi-Fi AP can be detected by Bluetooth slave device, where  $\delta$  is the time for handling the signal received from Wi-Fi devices. Let  $\lambda$  denote the signal strength threshold. That is, the signal strength on a channel higher than  $\lambda$  represents that the channel is busy. Let  $\beta_q$  be a Boolean variable indicating whether or not the signal strength received from channel  $c_q$  exceeds  $\lambda$ . If it is the case, a slave device  $b_j$  maintains a record  $(c_q, \varphi_q)$  in its interference table. Based on the channel scanning result, each slave device  $b_j$  maintains an

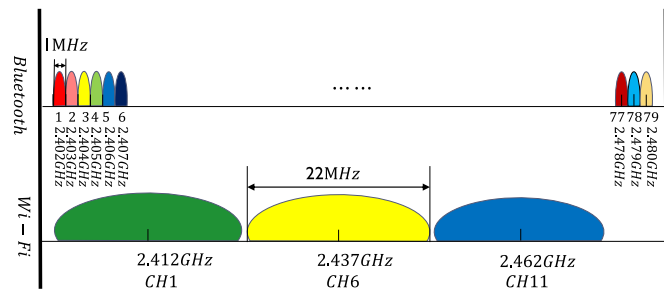


Fig. 1. Spectral overlap between Bluetooth and Wi-Fi.

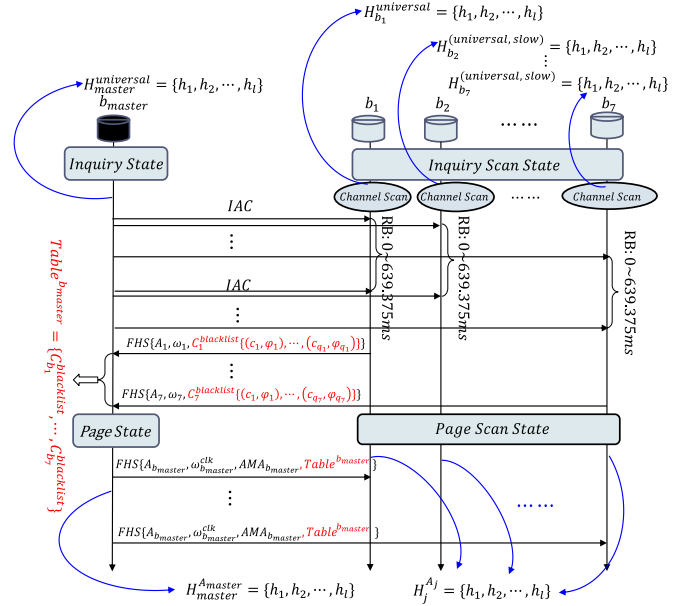


Fig. 2. Flows of the proposed Bluetooth connection protocol.

interference table  $C_j^{blacklist} = \{(c_1, \varphi_1), \dots, (c_q, \varphi_q)\}$  where  $\varphi_q$  denotes the signal strength of the scanned channel  $c_q$ . If  $\beta_q = 1$  is held,  $(c_q, \varphi_q)$  will be included in  $C_j^{blacklist}$ . To represent the hopping behavior, the following define the notation of hopping sequence. Let  $A_j$  denote the address of device  $b_j$  and  $H_j^{ppe}$  represent that a device  $b_j$  applies the hopping sequence with a type of “universal” or “ $A_j$ ”. If  $H_j^{universal}$  is applied, the device  $b_j$  performs the channel hopping according to the universal hopping sequence. By contrast, if  $H_j^{A_j}$  is applied, the device  $b_j$  follows the channel hopping sequence that is generated based on the address  $A_j$ .

According to the Bluetooth standard, the clock rate of Bluetooth chip should be at a rate of 320 Hz. The Bluetooth devices change its center frequency deterministically at a rate of 1600 Hz and the time slot is equal to 625  $\mu\text{s}$ . Let  $\pi(H_j, speed)$  denote the hopping channel behavior of device  $b_j$  that adopts hopping sequence  $H_j$  to execute channel hopping with a speed of “fast” or “slow”. Notation speed specifies the time period that device  $b_j$  stays on each channel. The Boolean parameter speed with “fast” or “slow” indicates that the hopping behavior is “fast” with a speed of two time slot or “slow” with a speed of 2048 time slot, respectively.

After executing the channel scan operation, all slaves  $\{b_1, b_2, \dots, b_7\}$  start to connect with  $b_{master}$ . The  $b_{master}$  intending to construct a piconet switches to the inquiry state. In the inquiry state, the master  $b_{master}$  adopts  $\pi(H_{master}^{universal}, fast)$  over 16 channels with a fast speed of 3200 hops/sec. To rendezvous with the master  $b_{master}$ , each slave  $b_j$  adopts  $\pi(H_j^{universal}, slow)$  over 16 channels a slow speed of 2048 time slot per channel. In the original Bluetooth standard (The Bluetooth Specification.), the master  $b_{master}$  initially sends inquiry access code (IAC) packets twice in each time slot for finding potential slave hosts. Upon receiving IAC packet, the slave  $b_j$  waits for a random back off duration, ranging from 0 to 1023 time slot, aiming to avoid the collision due to the more than one acknowledge received from more than one slave. Then slave  $b_j$  wakes up and waits for receiving the second IAC packet. At this moment, the slave still applies the slow hopping sequence. Upon receiving the second IAC packet, the slave  $b_j$  replies with a frequency hopping synchronization (FHS) packet that includes its Bluetooth address  $A_j$ , current clock  $\omega_j$  as well as the maintained channel black list  $C_j^{blacklist}$  which can utilize the undefined bits of

FHS packet to present the occupied Wi-Fi channels. The master  $b_{master}$  records the black list of channels, which can be derived by transferring the Wi-Fi channel to corresponding Bluetooth channels. After that, slave  $b_j$  switches to the page scan state and executes channel hopping with hopping behavior  $\pi(H_j^{A_j,slow})$ , which is generated based on its own  $A_j$ , waiting for receiving the master's FHS packet. Notice that the frequency-hopping of  $b_j$  can skip those channels maintained in the interference table. In the inquiry state, the master maintains a table  $Table^{b_{master}} = \{C_{b_1}^{blacklist}, C_{b_2}^{blacklist}, \dots, C_{b_7}^{blacklist}\}$ , which records every slave host's interference channels.

When  $b_{master}$  completes the inquiry state, which aims to rendezvous with each slave  $\{b_1, b_2, \dots, b_7\}$ , it switches to the page state accordingly. In the page state,  $b_{master}$  transmits an FHS packet, containing the Bluetooth address  $A_{b_{master}}$  and clock  $\omega_{master}$  of master  $b_{master}$  as well as the collected black list of  $Table^{b_{master}}$ , aiming to help slave hosts generating a common hopping sequence used during the connection state. On receiving the information sent from  $b_{master}$ , each slave host generates the hopping sequence  $H_{master}^A = \{h_1, h_2, \dots, h_l\}$  according to  $A_{b_{master}}$  but skips those channels maintained in  $Table^{b_{master}}$ .

By applying the proposed IAPE mechanism, we can reduce the interference before constructing the Bluetooth piconet. After the piconet construction, if the master suffered a terrible interference, the performance of the piconet will be highly affected. In the next section, this paper further presents the IAPR mechanism that restructures the piconet for improving the piconet performance.

#### 4. Interference Aware Piconet Restructuring (IAPR) mechanism

In a Bluetooth network, a piconet consists of a master and at most seven slaves. Each slave can only exchange data with the master in a piconet where the slave-to-slave direct communication is not allowed. When the master is suffering the interference, the performance of a piconet will be highly impacted. This proposed interference aware piconet restructuring (IAPR) mechanism aims to apply the role switching operation to cope with the interference problem. Role switching operation enables a slave to play a master role and take over all slaves of a piconet, reducing the impact of interference on transmissions. The change of master is complicated because the hopping sequences of all devices in the piconet should be accordingly changed. The Bluetooth supports HCI instructions to allow software to dynamically change the piconet structure according to Bluetooth standard (The Bluetooth Specification). More specifically, the Bluetooth standard defines HCI instructions, including *LMP\_switch\_req* and *LMP\_slot\_offset* to implement the role switch operations.

Recall that the hopping sequence is mainly generated based on the information of master's 48-bit Bluetooth address (BT\_ADDR)

and the clock of the new master. Therefore, each slave should obtain the new master's BT\_ADDR and clock information before establishing a new communication link between itself and the master. As shown in Fig. 3(a), device  $b_1$  is a master,  $b_2, b_3$  and  $b_4$  are slaves in a piconet. When master  $b_1$  is suffering a terrible interference by Wi-Fi devices, the master  $b_1$  cannot efficiently receive data from any slave. A role switching operation should be immediately executed to mitigate the phenomenon of interference. As shown in Fig. 3(b), the role switching operation enables that slave  $b_2$  replaces  $b_1$  to take over the piconet such that the traffic bottleneck caused by interference at device  $b_1$  might be removed.

To improve the throughput of a piconet, this paper chooses a proper slave to play the master role. The interference aware piconet restructuring (IAPR) mechanism consists of three phases, namely *Perceiving Phase*, *Evaluation Phase*, and *Role Switching Phase*. The *Perceiving Phase* determines the trigger criteria for executing the piconet role switching mechanism. As soon as the criteria are satisfied, the old master will initiate the *Evaluation Phase*. Each device in the piconet should evaluate its benefit for playing the role of a master. The *Role Switching Phase* aims to apply the role switching operations such that the device that has highest benefit will play the role of a master. The following describes the details of each phase.

##### 4.1. Perceiving phase

If the master suffers significant interference, the frequent retransmissions will be occurred, which degrades the network throughput. To be aware the frequent retransmissions, the master should collect the number of retransmissions of each packet to evaluate the degree of interference. Assume that there are  $n$  Bluetooth devices in a piconet  $C$ , represented by  $B = \{b_1, b_2, \dots, b_n\}, (n \leq 8)$ . Let  $b_{master}$  denote the master of piconet  $P$ . Let  $R_\theta$  denote the threshold of packet retransmissions. Let  $S_{succ} = \{s_1, s_2, \dots, s_y\}$  denote a set of the most recent received packets of  $b_{master}$ , where  $s_u$  is received earlier than  $s_{u+1}$ . Let  $r_u$  be the number of retransmissions of packet  $s_u$ . Upon receiving the packet  $s_u$ ,  $b_{master}$  should exam if the condition  $r_u > R_\theta$  holds. If it is the case, the master calculates the average number of retransmissions of the most recent  $y$  packets to make a decision whether or not the evaluation phase should be triggered. Let  $\bar{r}_{master}$  denote the average number of retransmissions of the most recent  $y$  packets successfully received by  $b_{master}$ . We have

$$\bar{r}_{master} = \frac{r_1 + r_2 + \dots + r_y}{y} \tag{7}$$

If  $\bar{r}_{master}$  is larger than the predefined restructuring threshold  $R_\theta$ ,  $b_{master}$  will initiate the evaluation phase. Otherwise, the master of piconet  $C$  will not be replaced and the  $b_{master}$  will abandon the perceiving phase.

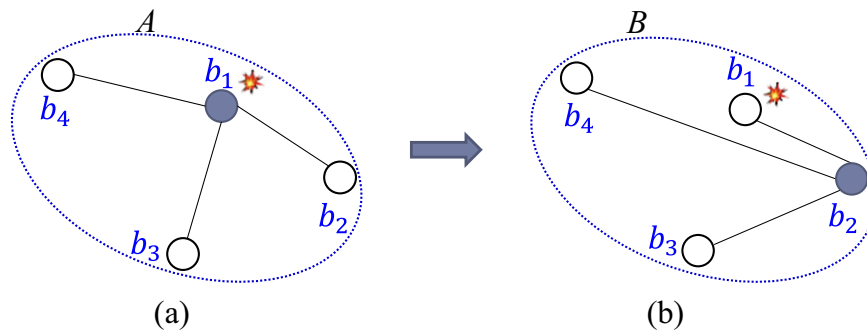


Fig. 3. Restructuring the topology of a Bluetooth Network. (a) Before piconet restructuring. (b) After piconet restructuring.

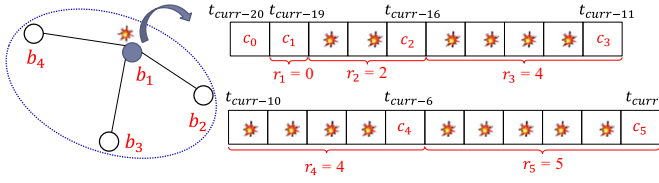


Fig. 4. Example of the perceiving phase.

To facilitate the details of perceiving phase, an example shown in Fig. 4 is used throughout this section. In Fig. 4, device  $b_1$  plays the master role and bridges all packets between the slaves  $b_2$ ,  $b_3$  and  $b_4$ . The threshold  $R_\theta$  and  $y$  are assumed to be 2 and 5, respectively. Let  $t_{curr}$  denote the current time. The master  $b_1$  received a packet  $c_5$  successfully at  $t_{curr}$ . In the perceiving phase, the master  $b_1$  exams whether or not the condition  $r_5 > R_\theta$  holds. The master  $b_1$  further calculates the average retransmission number of the most recent  $y=5$  packets to determine whether or not the evaluation phase should be triggered. As shown in Fig. 4, the retransmission numbers of packets  $c_1$ ,  $c_2$ ,  $c_3$ ,  $c_4$ , and  $c_5$  are 0, 2, 4, 4, and 5, respectively. By applying Exp. (7), the master's average number of retransmissions is  $\bar{r}_{master}=(0+2+4+4+5)/5=3$ . That is, the condition  $\bar{r}_{master} > R_\theta$  holds so that the master  $b_1$  will initiate the evaluation phase.

#### 4.2. Evaluation phase

In the perceiving phase, the master needs to be taken over because it suffers the significant interference. The evaluation phase aims to choose a proper slave to play the role of a master. The selection of slave to play the master role should consider two factors, including the interference and flow data volume. According to the two factors, the master can evaluate the benefit. First of all, the selection of slave should consider the "interference" factor. When the master suffers the significant interference, the benefit of master will be reduced dramatically because the number of retransmission increases. The old master should be replaced by the slave with the minimal interference, aiming to reduce the number of retransmissions. In addition to the interference factor, the selection of master should also consider the factor of flow data volume. According to the Bluetooth Spec, a slave can only exchange information with the master and it is not allowed to construct a direct communication link between slaves. Therefore, the source slave should firstly transmit packet to the master, then the master subsequently relays the packet to destination slave. Thus the change of master might cause that the lengths of some paths are changed. This also leads to the change of the total flow data volume in the new piconet.

According to the abovementioned two factors, the evaluation phase aims to derive an optimal topology. To accomplish this goal, the master should firstly evaluate the best benefit of piconet restructuring and then determine the best slave to play the role of new master. Based on the benefit comparison, if the evaluation benefit of the new master is better than that of the old piconet, the role switching phase will be initiated. Otherwise, the master will not be changed and the evaluation phase will be finished. The following presents the benefit evaluation procedure.

Let  $l_{ij}$  denote the directional edge from device  $b_i$  to device  $b_j$  in piconet  $C$ . Let  $F_{ij}^a$  denote the flow data volume from device  $b_i$  to device  $b_j$  in the piconet  $C$  in the most recent  $\hat{T}$  slots, where device  $b_a$  plays the master role and  $\hat{T}$  is a predefined time period. The value of  $F_{ii}^a$  should be zero, for all  $1 \leq i \leq n$ . Let path  $p_{ij}$  denotes the path from device  $b_i$  to device  $b_j$  in a piconet and  $|p_{ij}|$  denotes its

path length. If  $b_i$  and  $b_j$  are slaves in piconet  $C$ , we have  $|p_{ij}|=2$ , because the packets transmitted from  $b_i$  to  $b_j$  should be relayed by the master  $b_a$ . On the contrary, if one of  $b_i$  or  $b_j$  is master,  $|p_{ij}|=1$ . Let  $f_{ij}^1$  and  $f_{ij}^2$  denote the flow data volumes from  $b_i$  to  $b_a$  and from  $b_a$  to  $b_j$ , respectively. In the case of no transmission failure, the flow data volume  $F_{ij}^a$  can be obtained by Exp. (8),

$$F_{ij}^a = f_{ij}^1 + \alpha f_{ij}^2 \quad (8)$$

where  $\alpha$  denotes a Boolean available, representing whether or not the Bluetooth device  $b_j$  is a master. That is,

$$\alpha = \begin{cases} 0, & \text{if one of } b_i \text{ and } b_j \text{ is a master} \\ 1, & \text{otherwise} \end{cases} \quad (9)$$

Assume that some transmissions from  $b_i$  to  $b_j$  are failure. Let  $r_{ij}^1$  and  $r_{ij}^2$  denote the retransmission numbers from  $b_i$  to  $b_a$  and from  $b_a$  to  $b_j$ , respectively. Exp. (8) can be modified as shown in Exp. (10).

$$F_{ij}^a = f_{ij}^1 r_{ij}^1 + \alpha f_{ij}^2 r_{ij}^2 \quad (10)$$

Let  $F_a$  denote the total flow data volume of master  $b_a$ . We have

$$F_a = \sum_{\forall p_{ij}} F_{ij}^a \quad (11)$$

Therefore, the restructuring benefit  $\gamma^a$  can be obtained by the computation of Exp. (12).

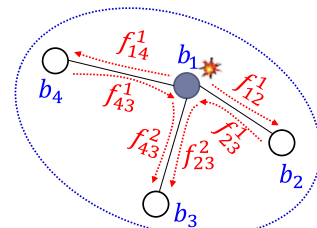
$$\gamma^a = 1 - F_a / F_{old\_master} \quad (12)$$

According to Exp. (12), the best selection of a new master should be

$$b_{new\_master} = \arg \max_{1 \leq a \leq n} \gamma^a \quad (13)$$

If  $b_{new\_master}$  is not the old master, the role switching phase will be triggered. Otherwise, the master will not be changed and the evaluation phase will be finished.

To facilitate the details of evaluation phase, an example shown in Fig. 5 is described in the following. As shown in Fig. 5, device  $b_1$  plays the master role and bridges all packets between the slaves  $b_2$ ,  $b_3$  and  $b_4$ . The example considers four recent flows: the first one is that flow  $p_{14}$  with 8 data units through link  $l_{14}$  and its retransmission number  $r_{14}^1$  is 2 from  $b_1$  to  $b_4$ ; the second one is that flow  $p_{12}$  with 9 data units through



Flow path	Link	Flow data volume	Number of retransmissions
$p_{14}$	$l_{14}$	$f_{14}^1=8$	$r_{14}^1=2$
$p_{12}$	$l_{12}$	$f_{12}^1=9$	$r_{12}^1=2$
$p_{43}$	$l_{41}$	$f_{43}^1=6$	$r_{43}^1=5$
	$l_{13}$	$f_{43}^2=6$	$r_{43}^2=2$
$p_{23}$	$l_{21}$	$f_{23}^1=10$	$r_{23}^1=6$
	$l_{13}$	$f_{23}^2=10$	$r_{23}^2=1$

Fig. 5. Example of the evaluation phase.

link  $l_{12}$  and its retransmission number  $r_{12}^1$  is 2 from  $b_1$  to  $b_2$ ; the third one is that flow  $p_{43}$  with 6 data units through links  $l_{41}$  and  $l_{13}$  from  $b_4$  to  $b_3$ . The retransmission numbers of  $r_{43}^1$  and  $r_{23}^2$  are 5 and 2, respectively; the fourth one is that flow  $p_{23}$  with 10 data units through links  $l_{21}$  and  $l_{13}$  from  $b_2$  to  $b_3$ . The retransmission numbers of  $r_{23}^1$  and  $r_{23}^2$  are 6 and 1, respectively. According to Exp. (11), the total flow data of master  $b_1$  is  $F_1 = f_{14}^1 \times r_{14}^1 + f_{12}^1 \times r_{12}^1 + f_{43}^1 \times r_{43}^1 + f_{43}^2 \times r_{43}^2 + f_{23}^1 \times r_{23}^1 + f_{23}^2 \times r_{23}^2 = 8 \times 2 + 9 \times 2 + 6 \times 5 + 6 \times 2 + 10 \times 6 + 10 \times 1 = 146$ .

Similarly, all slaves  $b_2, b_3$  and  $b_4$  should also evaluate their own total flow data to check if the role switching operation should be initiated. The following depicts the evaluations of total flows of all slaves  $b_2, b_3$  and  $b_4$ .

The total flow data of master  $b_2$  is  $F_2 = f_{14}^1 \times r_{14}^1 + f_{12}^2 \times r_{12}^2 + f_{12}^1 \times r_{12}^1 + f_{43}^1 \times r_{43}^1 + f_{43}^2 \times r_{43}^2 + f_{23}^1 \times r_{23}^1 = 8 \times 2 + 8 \times 2 + 9 \times 2 + 6 \times 2 + 6 \times 2 + 10 \times 2 = 94$ .

The total flow data of master  $b_3$  is  $F_3 = f_{14}^1 \times r_{14}^1 + f_{12}^2 \times r_{12}^2 + f_{12}^1 \times r_{12}^1 + f_{43}^1 \times r_{43}^1 + f_{43}^2 \times r_{43}^2 + f_{23}^1 \times r_{23}^1 = 8 \times 2 + 8 \times 2 + 9 \times 2 + 9 \times 2 + 6 \times 2 = 100$ .

The total flow data of master  $b_4$  is  $F_4 = f_{14}^1 \times r_{14}^1 + f_{12}^2 \times r_{12}^2 + f_{12}^1 \times r_{12}^1 + f_{43}^1 \times r_{43}^1 + f_{23}^1 \times r_{23}^1 + f_{23}^2 \times r_{23}^2 = 8 \times 2 + 9 \times 2 + 9 \times 2 + 6 \times 2 + 10 \times 2 + 10 \times 2 = 104$ .

According to Exp. (12), the restructuring benefits can be obtained accordingly.

$$\gamma^1 = 1 - \frac{F_1}{F_1} = 0$$

$$\gamma^2 = 1 - \frac{F_2}{F_1} = 1 - \frac{94}{152} = 0.38$$

$$\gamma^3 = 1 - \frac{F_3}{F_1} = 1 - \frac{100}{152} = 0.34$$

$$\gamma^4 = 1 - \frac{F_4}{F_1} = 1 - \frac{104}{152} = 0.32$$

As a result, according to Exp. (13), the new master is  $b_{new\_master} = \arg \max_{1 \leq a \leq 4} \gamma^a = b_2$ . Because the device  $b_2$  has the largest benefit, the old master  $b_1$  executes the following role switching phase.

### 4.3. Role switching phase

Without loss of generality, this section uses Fig. 6 as an example to illustrate the operations designed in the role switching phase. The formal algorithm is presented in the next section. As shown in Fig. 6(a), device  $b_1$  plays the master role and bridges all packets between the slaves  $b_2, b_3$  and  $b_4$ . According to the evaluation phase, device  $b_2$  has the maximal data flow volume in the piconet C. Therefore, it will be selected to play the role of a master in the restructured piconet. The old master  $b_1$  initiates the

execution of role switching phase.

The role switching phase aims to replace the old master  $b_1$  with device  $b_2$ . The change of master is complicated because that the hopping sequences of all devices in the piconet should be changed. The new hopping sequence is mainly generated based on the information of 48-bit BT\_ADDR and clock of the new master  $b_2$ . Therefore, each slave should derive BT\_ADDR and clock information of the new master  $b_2$  before establishing a new piconet topology. The following presents the details of role switching phase.

Firstly, the old master  $b_1$  sends a control message to the slaves  $b_2, b_3$  and  $b_4$ , aiming to reserve sufficient time slots for executing role switching operations and then notify the new master  $b_2$ . Upon receiving a control message, each slave that is not the new master responds an acknowledgment to device  $b_1$  and the new master  $b_2$  initiates a role switching request. Afterward, the master  $b_1$  replies the role switching response back to device  $b_2$ . Using the old hopping sequence, new master  $b_2$  respectively sends the time alignment LMP (link manager protocol) message to ask slaves  $b_1, b_3$  and  $b_4$  to delay for synchronizing the old piconet channel to new one and transfer the FHS packet, for frequency hop synchronization, with a new active member address and its 48-bit BT\_ADDR and clock information to each slave. The contents of 48-bit BT\_ADDR and clock information can help all slaves deriving the new hopping sequence of the new master  $b_2$ . Then each slave responds with the FHS acknowledgment to device  $b_2$ . The new master  $b_2$  and all slaves then apply the new hopping sequence. After that, the new master  $b_2$  sends devices  $b_3$  and  $b_4$  a POLL packet that is similar to the NULL packet but requires a confirmation from the recipient to verify the switch, thus rapidly connects with devices  $b_3$  and  $b_4$ . As shown in Fig. 6(b), device  $b_2$  take over all resource of master  $b_1$ , playing a master role in the restructured piconet.

### 4.4. IAPR algorithm

Fig. 7 shows the formal algorithm of IAPR. In Lines 1–7, the old master perceives the packet retransmission numbers and makes the decision whether or not it should initiate the Evaluation Phase. In Lines 8–18, the old master calculates the restructuring benefit of each device  $b_a$ , according to its traffic loads of the past  $\hat{T}$  slots. Lines 19–23 presents the procedure of Role Switching Phase.

Based on the execution of the proposed IAPR mechanism, a new piconet will be constructed, which is expected to have more benefits than the old piconet in terms of network throughput and average transmission delay.

Fig. 8 further presents the flow diagram of the proposed IAPR. In Fig. 8, several signals are exchanged among  $b_{old\_master}$ ,  $b_{new\_master}$  and  $b_{slave}$ . Initially, applying the old hopping sequence, the old master  $b_{old\_master}$  broadcasts the Evaluation\_Init packet to all slaves in the piconet C when  $\bar{r}_{old\_master}$  is greater than the threshold  $R_0$  in the perceiving phase. If the evaluated benefit of the restructuring of the new master is more than that of the old master, the old master  $b_{old\_master}$  broadcasts the Role\_Switch\_Init packet to all slaves in the

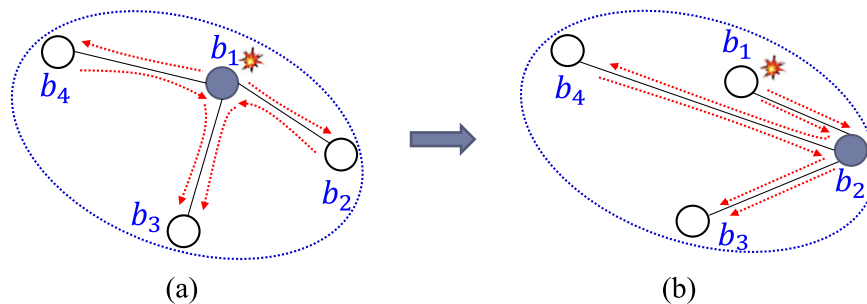


Fig. 6. Example of the role switching phase. (a) Before executing role switching. (b) After executing role switching.

**Algorithm:** Interference Aware Piconet Restructuring (IAPR)

- Input:** (1) an old piconet  $C$ ;  
 (2) the traffic of each flow in  $C$ ;  
 (3) the number of transmissions of each packet  $r_i$ ;  
 (4) retransmission threshold  $R_\theta$ .

**Output:** The new master  $b_{new\_master}$  of restructured piconet.

```

1. Perceiving Phase:
2.   if ( $r_y > R_\theta$ ) {
3.     calculates the average number of retransmission  $\bar{r}_{master}$ ,
4.     where  $\bar{r}_{master} = \frac{r_1+r_2+\dots+r_y}{y}$ 
5.   }
6.   if ( $\bar{r}_{master} \leq R_\theta$ ) {
7.     exit IAPR
8. Evaluation Phase:
9.   for each device  $b_a$  {
10.    calculate the total traffic load of piconet by
11.    
$$F_a = \sum_{\forall p_{ij}} F_{ij}^a, \text{ where } F_{ij}^a = f_{ij}^1 r_{ij}^1 + \alpha f_{ij}^2 r_{ij}^2$$

12.    calculate the benefit of device  $\gamma^a$ , where
13.    
$$\gamma^a = 1 - F_a / F_{old\_master}$$

14.   }
15.   find the new master  $b_{new\_master}$  by applying
16.   
$$b_{new\_master} = \arg \max_{1 \leq a \leq n} \gamma^a$$

17.   if ( $b_{new\_master} = b_{old\_master}$ )
18.     exit IAPR
19. Role Switching Phase:
20.    $b_{old\_master}$  sends  $CTL\_MSG$  to all slaves.
21.    $b_{new\_master}$  initiates role switch request.
22.    $b_{new\_master}$  sends  $LMP\_FHS$  and  $FHS$  packets.
23.    $b_{new\_master}$  sends  $POLL$  packet.
  
```

Fig. 7. The formal algorithm of IAPR mechanism.

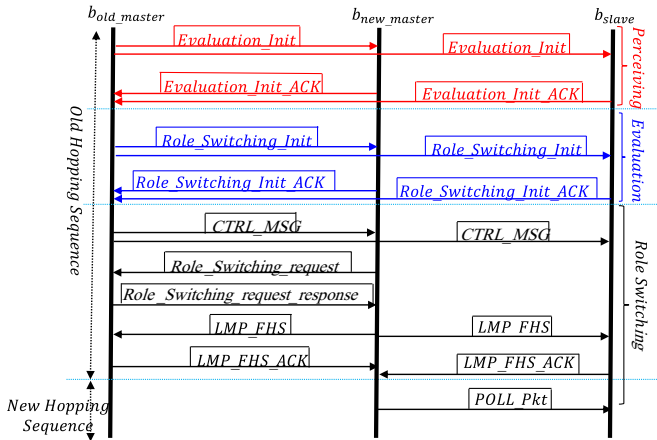


Fig. 8. Flow diagram of the proposed IAPR.

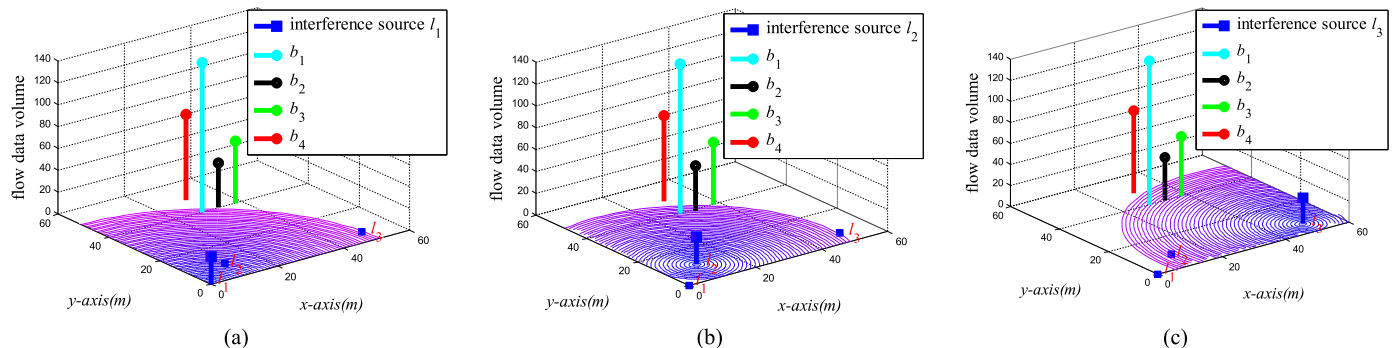


Fig. 9. Three experimental scenarios. (a) 1st Scenario: interference source is set at  $l_1$ . (b) 2nd Scenario: interference source is set at  $l_2$ . (c) 3rd Scenario: interference source is set at  $l_3$ .

evaluation phase. In the role switching phase, first, the old master  $b_{old\_master}$  sends  $CTRL\_MSG$  packet to the restructuring devices. Upon receiving the  $CTRL\_MSG$ , the new master  $b_{new\_master}$  sends  $Role\_Switch\_request$  packet to  $b_{old\_master}$ . The  $b_{new\_master}$  further sends  $LMP\_FHS$  packet to  $b_{old\_master}$  and  $b_{slave}$ . Each slave and old master responses with an ACK to the new master  $b_{new\_master}$ . The new master  $b_{new\_master}$  and all slaves then apply the new hopping sequence. After that, the new master  $b_{new\_master}$  sends each device  $b_{slave}$  with a  $POLL$  packet, which is similar to the  $NULL$  packet but aims to verify successes of the role switching operations.

## 5. Performance evaluation

This section investigates the performance evaluation of the *Original* and the proposed IAPR approaches by using MATLAB Simulink, where *Original* approach represents the Bluetooth Standard ([The Bluetooth Specification](#)). The environment is set as follows. The size of service region is set by  $60 \times 60 \text{ m}^2$ . Recall that the notation  $R_\theta$  denotes the threshold for executing the proposed IAPR approaches. Herein, the value of  $R_\theta$  is set by 5 retransmissions. Assume that the flow data volume of each Bluetooth device is stable in the piconet. Three locations of the interference sources, as marked by  $l_1$ ,  $l_2$  and  $l_3$ , were set in the service region. Fig. 9 represents the three experimental scenarios. The first, second and third scenarios set up the interference locations at locations  $l_1$ ,  $l_2$  and  $l_3$ , respectively. In the three scenarios, we use different colors, changing from blue to purple, to represent that the location farther from the interference source location has the weaker interference. There are four Bluetooth devices in a piconet, including  $b_1$ ,  $b_2$ ,  $b_3$  and  $b_4$ , where  $b_1$  plays a role of master and all the other

devices play the roles of slave. The  $z$ -axis presents the original flow data volume of each Bluetooth device. In the first scenario, as shown in Fig. 9(a), only master  $b_1$  is affected by the interference source, which is located at  $l_1$ . In the second scenario, as shown in Fig. 9(b), both devices master  $b_1$  and slave  $b_2$  are affected by the interference source, which is located at  $l_2$ . Similarly, Fig. 9(c) shows the third scenario where the three devices  $b_1$ ,  $b_2$  and  $b_3$  are affected by the interference source located at  $l_3$ .

The following discusses the performance comparisons of *Original* and the proposed IAPR approaches in terms of traffic overheads under different scenarios. A packet transmission might require many retransmissions if the interference causes transmissions failed. This indicates that the interference sources will cause packet retransmission and hence raise the traffic overheads. A good piconet restructuring algorithm should reduce the number of retransmissions and hence generates low traffic overheads. In Figs. 10–13, the traffic overheads of *Original* and the proposed IAPR are compared in three scenarios. The major differences in the three scenarios are the different locations of interference sources,

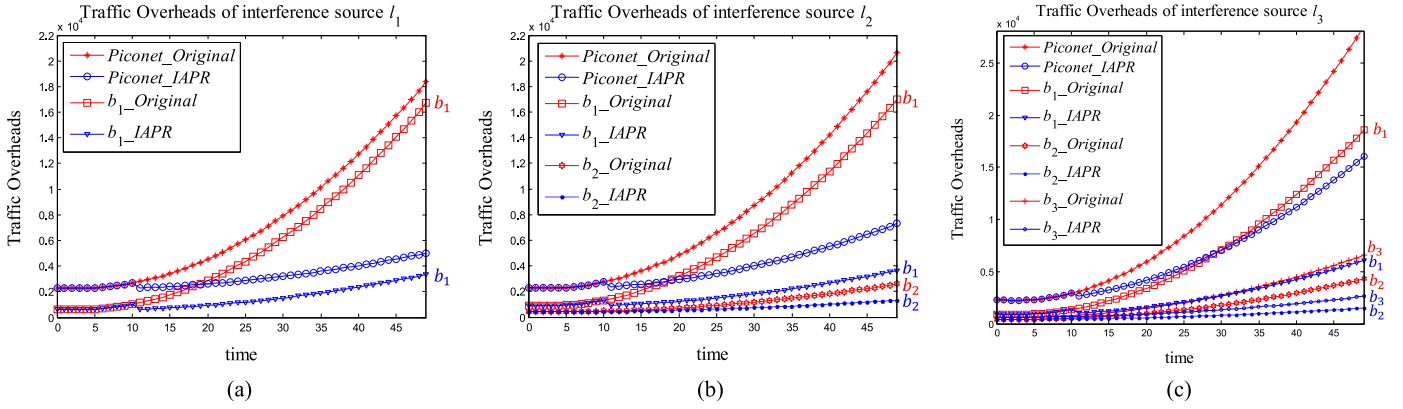


**Fig. 10.** Increasing curve with three interference sources. (a) Increasing curve with interference source  $l_1$ . (b) Increasing curve with interference source  $l_2$ . (c) Increasing curve with interference source  $l_3$ .

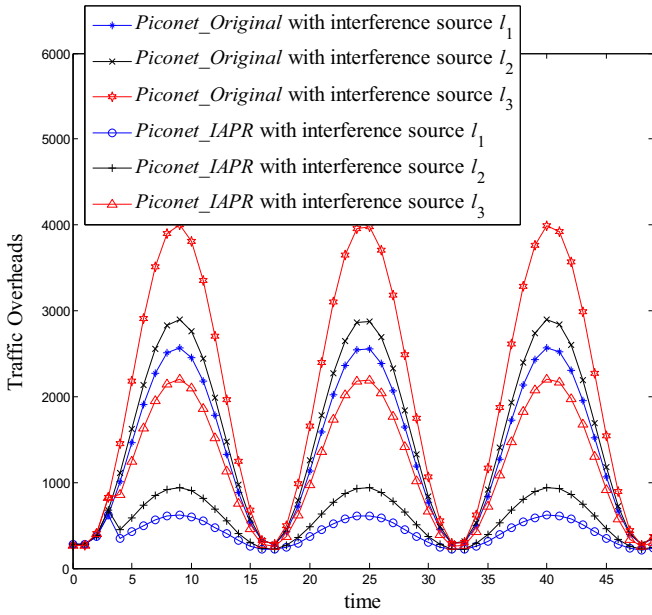


**Fig. 11.** The particular pattern periodically strength with three interference sources.

including locations  $l_1$ ,  $l_2$  and  $l_3$ . The legend of each compared curve will be represented as a form of combination containing two fields “devices” and “algorithm”. The first field could be one particular device such as  $b_1$ ,  $b_2$ ,  $b_3$  and  $b_4$ , which denotes the traffic overheads of devices  $b_1$ ,  $b_2$ ,  $b_3$ ,  $b_4$ . Moreover, the first field also can be “Piconet”, which denotes the traffic overheads of all devices. The second field, “algorithm”, can be either *IAPR* or *Original*, which means the applied algorithm. For instance, the curve named “Piconet\_Original” represents the total traffic overheads of the “Piconet”, which counts the traffic overheads of devices  $b_1$ ,  $b_2$ ,  $b_3$ , and  $b_4$  by applying the “Original” algorithm. Another instance is that the curve “ $b_1$ \_IAPR” denotes the traffic overheads of device  $b_1$  by applying the proposed *IAPR* algorithm.

Fig. 10 compares the two algorithms, *Original* and the proposed *IAPR*, in terms of traffic overheads. In Fig. 10(a), the interference source at location  $l_1$  is considered and hence only master  $b_1$  suffers the interference. As shown in Fig. 10(a), the traffic overheads of curves “Piconet\_Original” and “ $b_1$ \_Original” are similar. This occurs because that only device  $b_1$  suffers the interference. Therefore, most traffic overheads are generated from device  $b_1$ . Hence the traffic overheads of “Piconet” is similar to those of device  $b_1$ . Similarly, the curves “Piconet\_IAPR” and “ $b_1$ \_IAPR” are similar. In general, the proposed *IAPR* has smaller traffic overheads than the

*Original* algorithm. This indicates that applying the proposed *IAPR* algorithm can timely change the master, which has suffered the considerable interference.

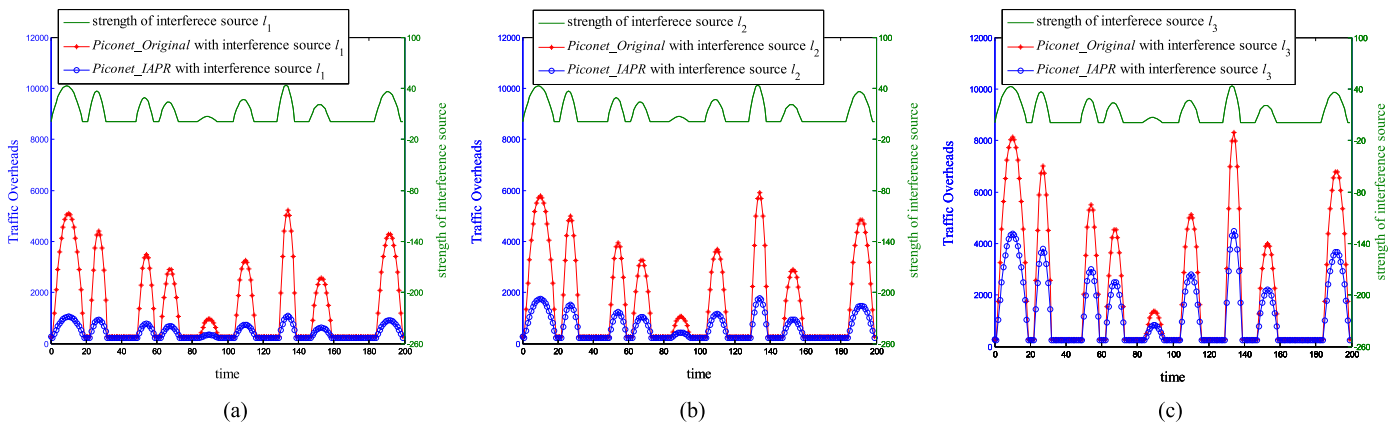
Fig. 10(b) compares the traffic overheads of devices  $b_1$ ,  $b_2$ , or *Piconet* in the environment of scenario two. That is, the interference source is set at location  $l_2$ , where the created interference only affect the traffic overheads of device  $b_1$  and  $b_2$ . The traffic overheads of devices  $b_3$  and  $b_4$  are ignored because that devices  $b_3$  and  $b_4$  are not affected by the interference in the second scenario. The sums of traffic overheads of curves “ $b_1$ \_Original” and “ $b_2$ \_Original” are sum of traffic overheads of curves “ $b_1$ \_IAPR” and “ $b_2$ \_IAPR” is closed to that of the curve “Piconet\_IAPR”. In general, the

proposed *IAPR* mechanism outperforms the existing *Original* mechanism in terms of traffic overheads of  $b_1$ ,  $b_2$  and piconet.

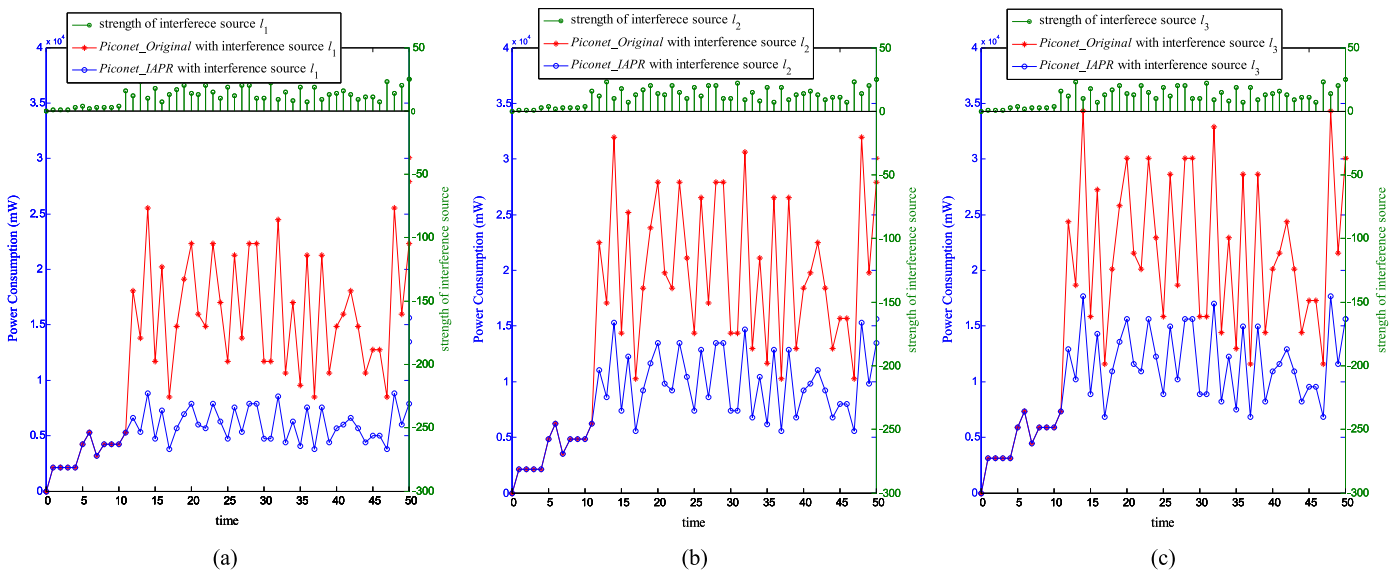
Similarly, Fig. 10(c) compares the traffic overheads of devices  $b_1$ ,  $b_2$ ,  $b_3$  and *Piconet* in the third scenario. That is, the interference source is set at location  $l_3$ , where the created interference only impacts on the traffic overheads of device  $b_1$ ,  $b_2$  and  $b_3$ . Since device  $b_4$  does not be affected by the interference in this scenario, this experiment does not consider  $b_4$ . In general, the proposed *IAPR* mechanism outperforms the existing *Original* mechanism in terms of traffic overheads.

Fig. 11 further compares the total traffic overheads of algorithms *Original* and the proposed *IAPR*. Since there are two algorithms applied in three different scenarios, there are totally six curves compared in Fig. 11. For those curves that apply the same scenario, the proposed *IAPR* outperforms *Original* in all cases in terms of traffic overheads. For instance, curve “Piconet\_IAPR with interference  $l_1$ ” has smaller traffic overheads than curve “Piconet\_Original with interference  $l_1$ ” in the first scenario. Similarly, curve “Piconet\_IAPR with interference  $l_2$ ” has smaller traffic overheads than “Piconet\_Original with interference  $l_2$ ” in the second scenario. Compare the curves that apply same algorithm in different scenarios. It is observed that the third scenario creates the largest overheads while the first scenario creates the smallest traffic overheads. This observations are valid no matter algorithms “Original” or “IAPR” are applied. For instance, curve “Piconet\_Original with interference  $l_3$ ” has the largest traffic overheads and curve “Piconet\_Original with interference  $l_1$ ” has the smallest traffic overheads by applying the *Original* algorithm. Similarly, curve “Piconet\_IAPR with interference  $l_3$ ” has the largest traffic overheads and curve “Piconet\_IAPR with interference  $l_1$ ” has the smallest traffic overheads by applying the proposed *IAPR* algorithm.

Fig. 12 compares *Original* and the proposed *IAPR* algorithms in terms of traffic overheads. Recall that the interference generated in Fig. 11 follows a particular pattern periodically. Different from Fig. 11, Fig. 12 is obtained by randomly choosing time point and randomly generating the interference strength at those chosen time points. All the other time periods are set with a constant



**Fig. 12.** Randomly generate the interference strength and time for three interference sources. (a) The interference strength and the corresponding time are randomly generated in the first scenario. (b) The interference strength and the corresponding time are randomly generated in the second scenario. (c) The interference strength and the corresponding time are randomly generated in the third scenario.



**Fig. 13.** Comparisons of distributed interferences with different strengths in three scenarios with different interference sources. (a) Verify the impact of distributed interferences on power consumption in the first scenario. (b) Verify the impact of distributed interferences on power consumption in the second scenario. (c) Verify the impact of distributed interferences on power consumption in the third scenario.

interference strength. Fig. 12(a) applies the first scenario as its experiment environment, where the interference source is set at location  $l_1$ . The green curve depicts the generated interference strength while the red and blue curves represent the traffic overheads of the *Original* and proposed *IAPR* algorithms, respectively. In general, the proposed *IAPR* outperforms *Original* in terms of traffic overheads in all cases. This occurs because that the proposed *IAPR* applies the *role switching* operations whenever the interference impact reaches the interference threshold. Hence the number of retransmissions can be substantially reduced. Fig. 12 (b) and (c) applies the second and third scenarios as the experiment environments, respectively. Compare the curves of Fig. 12(a), (b) and (c). It is observed that the curve in Fig. 12(c) has the largest traffic overheads while the curve in Fig. 12(a) has the smallest traffic overheads. This is valid no matter the *Original* algorithm or the proposed *IAPR* algorithm are applied. In fact, the curve in Fig. 12(c) has largest traffic overheads because that there are totally three Bluetooth devices, including  $b_1, b_2,$  and  $b_3,$  are interfered by the interference source located at  $l_3$ .

Recall that the continuous interference generated in Fig. 12

follows randomly choosing time points. Different from Fig. 12, several distributed interferences are generated in Fig. 13. Fig. 13 compares the *Original* and the proposed *IAPR* algorithms in terms of power consumption. It is assumed that the power consumption is 15.88 mW under the data production rate of 600 bytes/second (Balani, 2007). Fig. 13(a) applies the first scenario as its experiment environment where the interference source is set at location  $l_1$ . The green curve represents the generated interference strength while the red and blue curves represent the power consumptions of the *Original* and the proposed *IAPR* algorithms, respectively. It is notable that the interference strength generated during the time period (0, 10) is controlled to be small. As a result, the retransmission number is smaller than the threshold  $R_\theta$ .

Therefore, the power consumptions of *Original* and the proposed *IAPR* are similar during time period (0, 10). Since we enlarge the interference strength at time point 10, the retransmission number is increased and hence it exceeds the predefined retransmission threshold  $R_\theta$ . At this moment, the proposed *IAPR* algorithm applies the *role switching* operations to restructure the piconet topology. Hence the retransmission number substantially

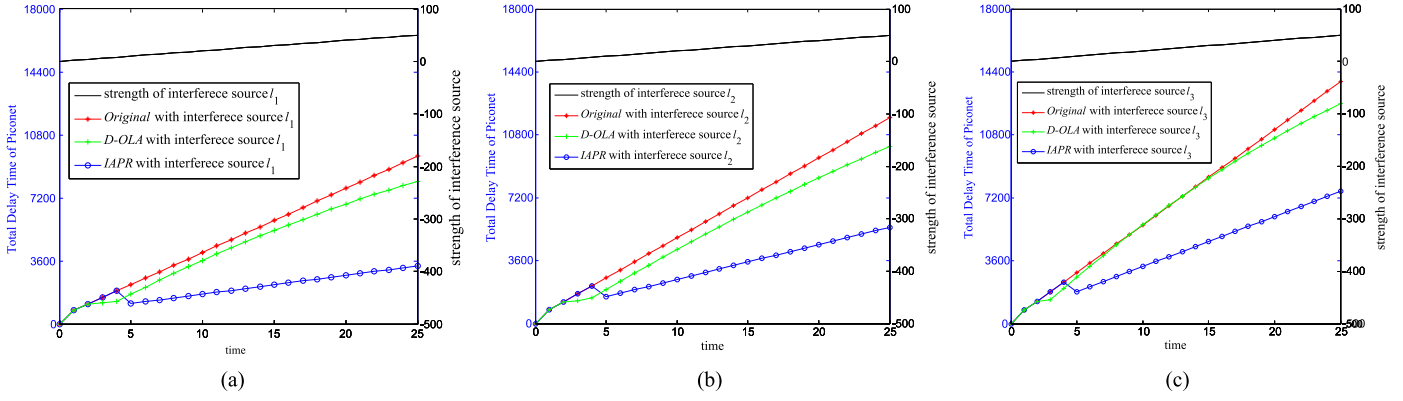


Fig. 14. Total delay time of a piconet with three interference sources. (a) Total delay time of a piconet with the interference source  $I_1$ . (b) Total delay time of a piconet with the interference source  $I_2$ . (c) Total delay time of a piconet with the interference source  $I_3$ .

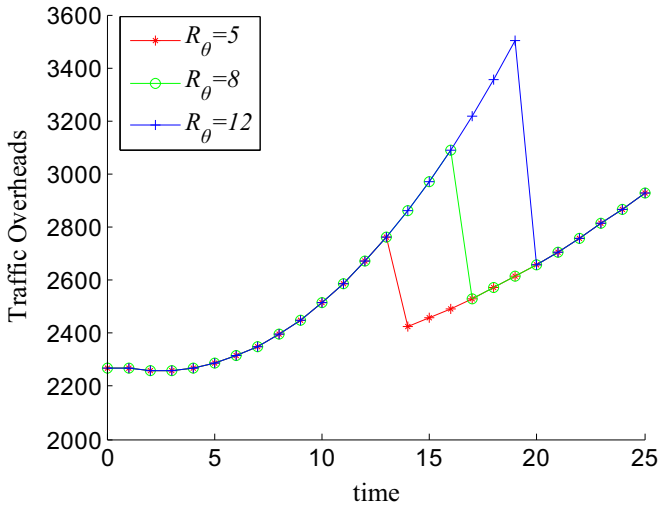


Fig. 15. Traffic overheads of different retransmissions threshold.

drops during the time period (10, 50). Fig. 13(b) and (c) has similar trends with Fig. 13(a). In general, the proposed IAPR outperforms Original in all cases in terms of power consumptions.

In addition, we further compare *Original*, *D-OLA* (Chiasserini and Rao, 2002) and the proposed *IAPR* algorithms in terms of total delay time of a piconet, as shown in Fig. 14(a), (b) and (c). The following describes the experimental environment. The black curve represents that the interference strength is increased with the increment of time. The packet arrival time for every device is 2.91 ms (Golmie et al., 2001). Fig. 14(a), (b) and (c) applies the first, second and third scenarios as its experiment environments, respectively. The red, green and blue curves depict the total delay time of the piconet by applying the *Original*, *D-OLA* and proposed *IAPR* algorithms, respectively. If the number of retransmissions is smaller than the threshold  $R_\theta$ , the *Original*, *D-OLA* and proposed *IAPR* algorithms have similar performance in terms of total delay time. However, the *IAPR* applies *role switching* operations to restructure the piconet at time point 5. Therefore, the proposed *IAPR* algorithm outperforms the *Original* and *D-OLA* algorithms in terms of total delay time. These observations can be found in Fig. 14(a), (b) and (c).

Fig. 15 compares different retransmissions threshold in terms of traffic overheads. The red, green and blue curves denote that the traffic overheads are increased with the increment of time in the retransmission threshold  $R_\theta$  of 5, 8 and 12, respectively. As shown in Fig. 15, the smaller retransmission threshold can save more traffic overheads of piconet.

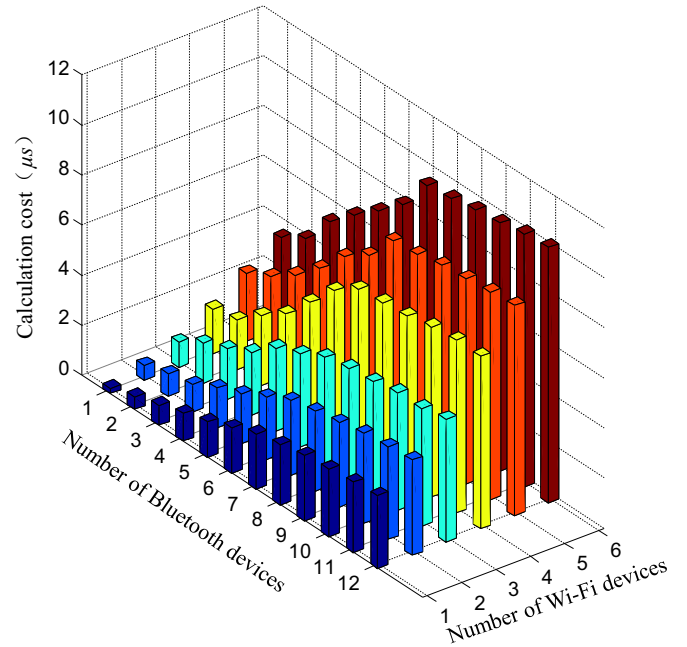


Fig. 16. Calculation cost of the proposed mechanism.

Fig. 16 presents the calculation cost of the proposed mechanism. The *x-axis* denotes the number of Wi-Fi devices, *y-axis* denotes the number of Bluetooth devices, and *z-axis* denotes the calculation cost (measured by  $\mu s$ ). In the experiments, a master is controlled to connect as most seven slaves. As shown in Fig. 16, the delay cost is increased when the numbers of Wi-Fi devices and Bluetooth devices are increased in the considered environment. This effect is especially significant when the number of Bluetooth devices grows from one to seven. However, when the number of Bluetooth devices is larger than seven, the number of slaves will not be increased in piconet. As a result, the calculation cost is increased slowly.

### 6. Conclusion

This paper presents novel link connection and topology restructuring mechanisms, called *IAPE* and *IAPR*, respectively, for Bluetooth personal area networks (PANs). The proposed *IAPE* helps a pair of master and slave devices constructing an efficient link by excluding the inappropriate channels in their hopping sequences. In addition, an *IAPR* mechanism is proposed to restructure the

topology of a piconet by applying role switching operations such that the new piconet can reduce not only the number of packet retransmissions but also energy consumptions of Bluetooth devices. Experiment results show that the proposed mechanisms outperform the traditional Bluetooth protocol in terms of traffic overheads, energy consumption as well as transmission delay.

## Acknowledgment

The paper is supported by National Natural Science Foundation of China (Grant no. 61472057), "Internet of things specialty" of Anhui Province (No. 2014tszy031), Chuzhou University Project (Nos. 2015GH08 and 2014KJ04), the Key Project of Anhui University Science Research (KJ2015A190) and the Technology R & D Program of Anhui Province of China (1501b042212).

## References

- Abdullah, M.F.L., Poh, L.M., 2011. Mobile robot temperature sensing application via Bluetooth. *Int. J. Smart Home* 5 (3), 39–48.
- Baccour, N., Koubãa, A., Mottola, L., et al., 2012. Radio link quality estimation in wireless sensor networks: a survey. *ACM Trans. Sens. Netw.* 8 (4), 34.
- Bakhsh, S.T., Hasbullah, H., Tahir, S., et al., 2012. A Flexible Relay Selection Technique for Bluetooth Scatternet. In: IEEE International Conference on Computer & Information Science (ICCIS); IEEE, Kuala Lumpur, Malaysia, pp. 718–722.
- Balani, R., 2007. Energy consumption analysis for Bluetooth, Wi-Fi and cellular networks. Networked & Embedded Systems Laboratory, NESL Technical Report TR-UCLA-NESL-200712-01.
- Chang, C.Y., Chang, H.R., 2006. Adaptive role switching protocol for improving scatternet performance in bluetooth radio networks. *IEEE Trans. Consum. Electron.* 52 (4), 1229–1238.
- Chiasserini, C.F., Rao, R.R., 2002. Coexistence mechanisms for interference mitigation between IEEE 802.11 WLANs and Bluetooth. In: Proceedings of Twenty-First Annual Joint Conference of the IEEE Computer and Communications Societies (INFOCOM); IEEE, New York, America, pp. 590–598.
- Golmie, N., Chevrollier, N., ElBakkouri, I., 2001. Interference aware Bluetooth packet scheduling. In: Global Telecommunications Conference (GLOBECOM'01); IEEE, San Antonio, TX, America, pp. 2857–2863.
- Gummadi, R., Wetherall, D., Greenstein, B., et al., 2007. Understanding and mitigating the impact of RF interference on 802.11 networks. *ACM SIGCOMM Comput. Commun. Rev.* 37 (4), 385–396.
- Jeon, W., Han, S., Choi, J.W., et al., 2013. Harnessing self-cancellation for coexistence of Wi-Fi and Bluetooth. In: IEEE 5th International Conference on Ubiquitous and Future Networks (ICUFN). IEEE, Da Nang, Vietnam, pp. 294–299.
- Lavric, A., Popa, V., Finis, I., Gaitan, A.M., Petrariu, A.I., 2012. Packet error rate analysis of IEEE 802.15.4 under 802.11g and Bluetooth interferences. In: IEEE 9th International Conference on Communications (COMM). IEEE, Bucharest, Romania, pp. 259–262.
- Lakshminarayanan, K., Seshan, S., Steenkiste, P., 2011. Understanding 802.11 performance in heterogeneous environments. In: Proceedings of the 2nd ACM SIGCOMM workshop on Home Networks; ACM, Toronto, Canada, pp. 43–48.
- Lee, S.H., Kim, H.S., Lee, Y.H., 2012. Mitigation of co-channel interference in Bluetooth piconets. *IEEE Trans. Wirel. Commun.* 11 (4), 1249–1254.
- Lee, J.S., Su, Y.W., Shen, C.C., 2007. A comparative study of wireless protocols: Bluetooth, UWB, ZigBee, and Wi-Fi. In: The 33rd Annual Conference of the IEEE Industrial Electronics Society (IECON). IEEE, Taipei, Taiwan, pp. 46–51.
- Ophir, L., Bitran, Y., Sherman, I., 2004. Wi-Fi (IEEE 802.11) and Bluetooth coexistence: issues and solutions. In: IEEE 15th International Symposium on Personal, Indoor and Mobile Radio Communications (PIMRC). IEEE, Barcelona, Spain, pp. 847–852.
- The Bluetooth Specification, (<http://www.bluetooth.org/>).
- Wang, X.H., Iqbal, M., 2006. Bluetooth: opening a blue sky for healthcare. *Mob. Inf. Syst.* 2 (2–3), 151–167.
- Yoon, S.U., Murawski, R., Ekici, E., et al., 2010. Adaptive channel hopping for interference robust wireless sensor networks. IEEE International Conference on Communications (ICC); IEEE, Cape Town, South Africa, pp. 1–5.